



Weak surface temperature effects of recent reductions in shipping SO₂ emissions, with quantification confounded by internal variability

Duncan Watson-Parris¹, Laura J. Wilcox², Camilla W. Stjern³, Robert J. Allen⁴, Geeta Persad⁵, Massimo A. Bollasina⁶, Annica M. L. Ekman⁷, Carley E. Iles³, Manoj Joshi⁸, Marianne T. Lund³, Daniel McCoy⁹, and Daniel M. Westervelt¹⁰, Andrew Williams¹¹, Bjørn H. Samset³

¹Scripps Institution of Oceanography and Halicioğlu Data Science Institute, UC San Diego

²National Centre for Atmospheric Science, Department of Meteorology, University of Reading

³CICERO Center for International Climate Research, Oslo

⁴Department of Earth and Planetary Sciences, University of California, Riverside

⁵Jackson School of Geosciences, University of Texas at Austin

⁶School of GeoSciences, University of Edinburgh, UK

⁷Department of Meteorology and Bolin Centre for Climate Research, Stockholm University

⁸Climatic Research Unit, School of Environmental Sciences, University of East Anglia, UK

⁹University of Wyoming

¹⁰Lamont-Doherty Earth Observatory, Columbia University

¹¹Princeton University

Correspondence to: Duncan Watson-Parris (dwatsonparris@ucsd.edu)

Abstract.

In 2020 the International Maritime Organization (IMO) implemented strict new regulations on the emissions of sulphate aerosol from the world's shipping fleet. This can be expected to lead to a reduction in aerosol-driven cooling, unmasking a portion of greenhouse gas warming. The magnitude of the effect is uncertain, however, due to the large remaining uncertainties in the climate response to aerosols. Here, we investigate this question using an 18-member ensemble of fully coupled climate simulations evenly sampling key modes of climate variability with the NCAR CESM2 model. We show that while there is a clear physical response of the climate system to the IMO regulations, including a surface temperature increase, we do not find global mean temperature influence that



is significantly different from zero. The 20-year average global mean warming for 2020-2040 is $+0.03\text{ }^{\circ}\text{C}$, with a 5-95% confidence range of $[-0.09, 0.19]$, reflecting the weakness of the perturbation relative to internal variability. We do, however, find a robust, non-zero regional temperature response in part of the North Atlantic. We also find that the maximum annual-mean ensemble-mean warming occurs around a decade after the perturbation in 2029, which means that the IMO regulations have likely had very limited influence on observed global warming to date. We further discuss our results in light of other, recent publications that have reached different conclusions. Overall, while the IMO regulations may contribute up to at $0.16\text{ }^{\circ}\text{C}$ $[-0.17, 0.52]$ to the global mean surface temperature in individual years during this decade, consistent with some early studies, such a response is unlikely to have been discernible above internal variability by the end of 2023 and is in fact consistent with zero throughout the 2020-2040 period.

Introduction

Anthropogenic aerosols play a complex and dual role in Earth's climate system. On the one hand, they contribute to atmospheric pollution, adversely affecting air quality and public health. On the other hand, they mostly exert a net cooling effect on the climate by increasing the albedo, or reflectivity, of the atmosphere, thereby reducing the amount of solar radiation that reaches the Earth's surface (Bellouin et al., 2020). Sulphate aerosols, for instance, scatter sunlight, directly and enhance cloud brightness by increasing the number of water droplets in clouds, further reflecting sunlight away from the Earth (e.g. Albrecht, 1989; Twomey, 1974). Anthropogenic aerosol emissions thereby currently induce a global average cooling which (partially) offsets greenhouse gas driven warming by around $0.5\text{ }^{\circ}\text{C}$ $[0.22\text{ to }0.96]$ compared to pre-industrial times (Forster et al., 2021). The magnitude of aerosol cooling is a key uncertainty in climate science and hinders our ability to accurately predict the magnitude and timing of future warming (Watson-Parris & Smith, 2022).



Environmental and health concerns associated with anthropogenic aerosols have led to international efforts to reduce their emission, with potentially significant consequences for the climate (Wall et al., 2022). In January 2020, the International Maritime Organization (IMO) took a significant step in this direction by implementing stringent regulations to curb sulphur dioxide (SO_2 ; a precursor for sulphate aerosol) emissions from the global shipping fleet (IMO 2019), which at the time contributed around 14% of all anthropogenic sources of these pollutants (Christensen et al., 2022). Given the substantial share of global trade transported by sea, and the corresponding volume of emissions from shipping, the impact of these regulations on the global climate system was anticipated to be notable, and to provide a useful experiment to quantify broader aerosol impacts (Christensen et al., 2022). Similar regulatory efforts in other sectors, and national efforts in major industrial nations such as China (Li et al., 2017; Samset et al., 2019; van der A et al., 2017), also aim to improve air quality by reducing emissions of SO_2 and other aerosol precursors or species, thereby posing a challenge to climate scientists: to quantify and predict how these reductions will influence Earth's energy balance and the ongoing rate and pattern of warming.

While focussed studies have found evidence of the effect of the change in shipping emissions on cloud brightness (Diamond, 2023; Watson-Parris et al., 2022), it is challenging to discern any signal in large-scale cloud properties because the observed covariability does not always flow causally from the observed microphysical properties (Glassmeier et al., 2021; Stevens & Feingold, 2009). The instantaneous radiative forcing due to aerosol-cloud interactions from the 2020 change in shipping emissions is estimated to be 0.5 W m^{-2} in the annual mean within shipping corridors. Best estimates of the global mean effective radiative forcing (ERF) resulting from an 80% drop in shipping emissions range from 0.035 to 0.15 W m^{-2} across multiple models and methodologies (Gettelman et al. 2024; Skeie et al., 2024; Yoshioka et al., 2024). Yuan et al. (2024) report a forcing of 0.2 W m^{-2} averaged over the global ocean only, which is consistent with these global estimates.



70

71 A possible discernible climate influence of the IMO regulations became a topic for discussion in 2023, when
72 observed global mean surface temperatures (GMST) set a record. The 2023 GMST anomaly exceeded predictions
73 based on long-term climate change trends and internal variability, including the El Niño-Southern Oscillation
74 (ENSO), by more than 0.2°C, causing speculation that the reduction in SO₂ emissions from shipping could be one
75 of the driving factors (Schmidt, 2024). Based on the estimates of ERF given above, however, calculations with
76 simple energy balance models (EBMs) suggest that the warming associated with shipping changes since 2020 is
77 unlikely to exceed 0.05 °C by 2023, with a long-term response of 0.07K (Gottelman et al., 2024). A weakness of
78 the EBMs in this case, however, is that they generally assume a spatially homogeneous forcing and thus cannot
79 account for the spatial heterogeneity in ocean feedbacks or climate responses to aerosol forcing, which is known
80 to be substantial (Persad & Caldeira, 2018; Shindell & Faluvegi, 2009; Westervelt et al., 2020).

81

82 To provide a quantitative estimate of the magnitude and pattern of the climate response to the IMO shipping
83 regulations, and the role it may have played in recent record surface temperatures, it is therefore crucial to also
84 have estimates using fully coupled Earth System Models (ESMs), that take into account a broad range of aerosol-
85 climate interactions and their spatial heterogeneity, as well as internal variability and its potential feedback on
86 transient climate forcing. The latter means that it is necessary to use an ensemble of model simulations that is
87 sufficiently large to discern a statistically significant temperature response to a weak perturbation. Even with
88 ESMs, structural uncertainty and ensemble size create disagreement, as evidenced by recent studies of surface
89 warming estimates due to shipping emission reductions. For instance, Yoshioka et al. (2024) found a global mean
90 temperature increase of 0.04K, averaged over 2020 to 2049, in response to a 0.13 W m⁻² ERF in HadGEM3-GC3.1,



while Quaglia & Visioni (2024) found a global temperature increase of 0.2 °C by 2030 in response to an approximately 0.2 W m⁻² ERF in CESM2 (for a 90% reduction in shipping emissions).

Here, we present estimates of the transient surface temperature implications of the recent IMO regulations, using a large (18 member) ensemble of fully coupled transient simulations with the Community Earth System Model version 2 (CESM2). We show the ensemble mean response over time and discuss the implications of the sample size for the ability to quantify any forced warming. Also, as it is conceivable that the current specific phases of ENSO and Atlantic Multi-decadal Oscillation (AMO) could be particularly (in)sensitive to radiative perturbations in the shipping corridors (e.g. Wang et al., 2022), we have designed the ensemble to sample different modes of climate variability. Finally, as there have already been a range of studies quantifying the temperature response to the IMO regulations leading to differing, if not opposite, conclusions, we provide a broader discussion on the challenges and limitations of disentangling the effect of shipping emissions using currently available climate modelling methodologies.

Methods

CESM2 (Danabasoglu et al., 2020) consists of the Community Atmosphere Model version 6 (CAM6; Bogenschutz et al., 2018), the Parallel Ocean Program version 2 (POP2; Danabasoglu et al., 2012), the Community Land Model version 5 (CLM5; Lawrence et al., 2019), and the Community Ice Code version 5 (CICE; Hunke et al., 2015). Aerosols in CAM6 are represented by the four-mode version of the Modal Aerosol Module (MAM4; Liu et al., 2016). We note that 2.5% of SO₂ emissions from the international shipping sector are emitted as sulphate aerosol at the surface level and into the accumulation mode (Emmons et al., 2020). The cloud microphysics scheme is



version 2 of the Morrison-Gottelman scheme (Gottelman & Morrison, 2015). Simulations are performed at approximately 1° horizontal resolution.

Our baseline experiments come from archived simulations performed as part of the CESM2 Large Ensemble (CESM2-LE) Project (Rodgers et al., 2021). From 2015 onwards, CESM2-LE uses aerosol/precursor gas emissions (including SO₂/SO₄ from international shipping), land use changes, and greenhouse gas concentrations from the Shared Socioeconomic Pathway 3-7.0 (SSP3-7.0; O'Neill et al., 2016). Our perturbation experiments are initialised from the CESM2-LE baseline experiments beginning in 2015 and integrated through 2040. The perturbation simulations are identical to the baseline simulations, except for a uniform 80% reduction in SO₂/SO₄ emissions from international shipping starting in 2020 (consistent with the IMO regulations) and extending through 2040. Thus, taking a difference (perturbation minus baseline) isolates the effects of the decrease in SO₂ emissions from international shipping.

CESM2 has a relatively strong anthropogenic aerosol forcing when quantified in isolation, and a high climate sensitivity compared to other ESMs (see Figure 1; Schlund et al., 2020; Zelinka et al., 2023). Its oceanic response has also been shown to be particularly sensitive to aerosol emissions (Fasullo et al., 2023; Hassan et al., 2021). For this particular perturbation however, CESM2 shows a similar radiative forcing to other ESMs (Skeie et al., 2024). Our model setup is the same as the one used for CESM2 in Gottelman et al. 2024 who report an ERF of 0.11 Wm⁻² for a 100±25% reduction in shipping SO₂ emissions. This places CESM2 near the mean of the ERF estimates recently provided (Skeie et al., 2024; Gottelman et al. 2024).



To help understand the possible importance of the imposed shipping emissions perturbation relative to internal climate variability, we perform 18 ensemble simulations. These ensemble members all use CESM2-LE realisations that feature 11-year running mean smoothed CMIP6 biomass burning emissions, including members 1011-001, 1031-002, 1051-003, 1091-005, 1111-006, 1131-007, 1151-008, 1171-009, 1191-010, 1231-011, 1231-012, 1231-016, 1231-018, 1251-012, 1281-017, 1281-020, 1301-015, 1301-017. Recent satellite data introduces more interannual variability into the biomass burning dataset than data sources used before 1997 and after 2014, so smoothing reduces the variability in biomass burning fluxes over 1990–2020 (Fasullo et al., 2022). Furthermore, to help understand the possible importance of dominant modes of climate variability (e.g., ENSO and AMV) to the climate impacts associated with the shipping perturbation, 8 of the above ensemble members feature ENSO neutral conditions, 5 feature ENSO positive conditions and 5 feature ENSO negative conditions. The AMV index is also evenly sampled in the ensemble, for each ENSO state, and spans -0.15 to 0.15.

The simulated responses are compared to observed SST changes, diagnosed from the HadCRUT v5.0.2 analysis (Morice et al., 2021). We fit a locally weighted regression (LOESS) model over time to each 5x5 degree grid-cell to model the long-term SST trends (2020-2040), and then subtract this to discern the anomaly in 2023.

In the following, unless otherwise specified, estimates for surface temperature change are for the period 2020-2040. All significance tests are performed using a two-sided Student's t-test for the null hypothesis that two independent samples (drawn from two distributions with equal variance) have identical average (expected) values.



Results

Figure 2a shows the relative change in near-surface SO_2 concentration in the reduction scenario compared to baseline and demonstrates that the majority of the changes in near-surface SO_2 occur over the Northern Hemisphere oceans and in particular over the North Atlantic and North-East Pacific – clearly aligned with the main international shipping routes. Figure 2b shows the change in near-surface SO_2 concentrations over the simulation period both globally and over the North Atlantic. The gradual reduction in the change over the period is due to the underlying shipping emission reductions in the baseline SSP3-7.0 scenario.

Despite these wide-spread and regionally significant changes in SO_2 concentrations (and corresponding SO_4 concentrations, not shown), the temperature response in these simulations is negligible. Based on our sample of 18 simulations, we calculate a global, 20-year mean surface temperature change from the IMO regulations of +0.03 °C, with a 5-95% confidence range of [-0.09, 0.19]. Figure 3a shows the temperature change with respect to the baseline simulations as a global mean and over the North Atlantic, neither of which show significant spatial-mean warming over the 20-year study period. In fact, over the first five years there is no statistically robust change in temperature found anywhere on the globe (see Fig 3b), demonstrating the low strength of the perturbation with respect to the model's simulated internal variability of the Earth system. Averaging over 20 years, a robust localized signal starts to appear during 2020-2040 in a small region of the North Atlantic (see Fig 3c) where there is a statistically significant local warming of around 0.2°C. Figure 3d shows that the anomalous warming observed in the region in 2023 (see Methods) does broadly correspond with the pattern of simulated warming in response to the IMO regulations, but only as discerned after 20 years, visualised in Fig. 3e (which is a close-up of 3c).



Despite some degree of similarity between the recent observed anomalous warming and the simulated temperatures shown in Fig 3e, the timescales do not match. The observed anomalies occurred three years after the emissions changes, while the average model response over the first five years (2020-2025) shows no significant warming in the region (Fig. 3b). As noted above, it is possible that the particular phase of ENSO or AMO could have made the North Atlantic particularly susceptible to such a perturbation in this short period of time in observations, but by sub-sampling our ensemble based on these characteristic modes we still find no evidence that the shipping emissions changes could have contributed significantly to the observed global temperature changes (see Fig. 4).

As mentioned above, detecting the climate impacts of a relatively small externally forced perturbation, such as the estimated global top-of-atmosphere radiative forcing associated with the IMO shipping regulations (e.g., $+0.12 \pm 0.03 \text{ Wm}^{-2}$; Gettelman et al. 2024), is complicated by the influence of internal climate variability (Deser et al., 2012, 2020). Figure 5 shows the actual evolution of our 18 ensemble members, with and without the IMO regulations, compared to the HadCRUT5 global surface temperature anomaly data series. The observed evolution is clearly within the range sampled by CESM2, in both emission scenarios. This difficulty is compounded over smaller (e.g., regional) spatial scales and shorter (e.g., decadal) time scales. The ability to robustly separate and quantify a forced signal in the climate system is the goal and motivation of “large-ensembles” (e.g. Kay et al., 2015; Kirchmeier-Young et al., 2017; Maher et al., 2019; Rodgers et al., 2021; Simpson et al., 2023), whereby dozens or more independent climate model ensemble members are generated using identical external forcing but different initial climate states. Since ensemble members will in general feature different timing of internal climate variability—which essentially represents noise (i.e., the component of the signal that is not externally forced)—averaging over a larger number of ensemble members reduces such noise, allowing for a more robust quantification of the externally forced signal.



194
195 Figure 6 shows the important influence of internal climate variability to the global mean temperature response (ΔT)
196 in our CESM2 shipping perturbation experiments, as well as the importance of having a sufficient ensemble size
197 to robustly detect a forced response. Fig. 6a shows the impact of randomly selecting N of our 18 ensemble
198 members with replacement (i.e. a bootstrapping analysis). For each combination we calculate the corresponding
199 ensemble global mean temperature response. The figure shows the results for $n=1000$ samples. For small N , the
200 spread in the ensemble mean ΔT is quite large (approximately -0.09 to 0.125 °C for $N = 5$). For $N = 10$, the spread
201 is reduced, but it still exceeds ± 0.05 °C. As N continues to increase, however, the spread converges to our 18-
202 ensemble member ΔT .

203
204 To further illustrate the importance of ensemble size when dealing with perturbations that have weak responses
205 relative to internal variability, Figure 6b-d show example combinations of 10 unique ensemble members (as used
206 e.g. by Quaglia & Vioni, 2024). Statistical testing and hatching is done as for our Figure 3 (see Methods). Fig.
207 6b shows a 10-member combination consistent with our 18-member mean response ($\Delta T = 0.03$ °C). 6c and 6d
208 show 10-member combinations with ΔT at the edges of, but still within, the 9-95% confidence interval ($\Delta T = \pm 0.05$
209 °C).

210
211 While panels b-d of Figure 6 all represent deliberate picking of ensemble members, the analysis illustrates how,
212 even with a decently sized ensemble of 10 members, one could conclude that the IMO shipping regulations may
213 lead to substantial global mean warming or global mean cooling. This illustrates the importance of internal climate
214 variability in detecting a global mean temperature response associated with the IMO shipping regulations, and the
215 importance of a sufficiently large ensemble size to reduce the risk of spurious conclusions. We note that our choice



of 18 ensemble members, as with most experimental designs, also represents a trade-off between additional information gained versus increased computational expense. Clearly, however, a moderately large ensemble size of 10—which has been shown to be sufficient in some contexts (e.g. Monerie et al., 2022)—is not sufficient to make robust claims regarding the impact of shipping SO₂ reductions on global mean temperature, in particular during its early transient evolution.

Discussion and conclusions

The strict new fuel regulations introduced by the IMO provided a valuable experiment to better understand the role of changing anthropogenic aerosol in the climate system, particularly as an analogue to other, current and future, efforts to improve air quality globally. Using an 18-member ensemble of simulations from CESM2, we find that the global temperature response to the IMO regulations that came into force in 2020 is +0.03 °C, with a 5-95% confidence range of [-0.09, 0.19], for the period 2020-2040. This result, which is consistent with a null hypothesis of no discernible global mean temperature response, is at the low end of other estimates of this warming effect, from simple energy balance models (Gettelman et al., 2024; Yuan et al., 2024) and global climate models (Quaglia & Vioni, 2024; Yoshioka et al., 2024), which suggested global warming between 0.04 °C (Yoshioka et al., 2024) and 0.2 °C (Quaglia & Vioni, 2024) associated with the shipping regulations over decadal timescales. To understand the differences between these conclusions and to explain why our analysis provides an important bound on the role of shipping emissions changes in recently observed temperature extremes, it is necessary to discuss in some detail the methodologies and framings behind the other results.



Some recent studies of the climate impact of the IMO regulations used EBMs to calculate the global temperature response from the effective radiative forcing (Gettelman et al., 2024; Yuan et al., 2024). These simple models are useful in many situations, notably for comparing the climate implications of known emissions from industrial sectors, regions or scenarios. However for absolute climate impacts they require substantial assumptions to be made about the sensitivity and timescale of the responses, and – critically - do not account for regional heterogeneity of responses or climate feedbacks such as influences on ocean circulation or sea ice, or internal variability. Ocean feedbacks may be particularly important in the case of shipping emission changes which are focussed over the Northern Hemisphere oceans, where it is conceivable that the ocean mixed layers may warm more efficiently than e.g. the Southern Ocean (e.g. Ma et al., 2020). Region-specific cloud responses and teleconnections to aerosol changes over Northern Hemisphere oceans may also differ from those to e.g. sulphur emission changes in Asia (Burney et al., 2022; Persad & Caldeira, 2018), which tend to dominate the total global response to recent sulphur emission changes used to calibrate simple EBMs. Coupled climate models provide estimates of the temperature response to the IMO regulations that take such feedbacks and pattern dependencies into account.

Despite the differences in the approach, our estimate of the global warming due to the IMO regulations is similar to Gettelman et al. (2024)'s estimate of 0.07 °C by 2030, which is based on the FaIR EBM. The EBM approach taken by Yuan et al. (2024), however, which diagnoses a global temperature anomaly of 0.17 °C at equilibrium overstates the response to their forcing by a factor of 1.4. This is because Yuan et al. (2024) calculate a global temperature response using a global climate feedback parameter, but using an ocean-area mean ERF. A global feedback parameter should be used with a global forcing in this context, which would reduce their forcing and temperature estimates by a factor of 0.7, the fraction of global area that is ocean, from 0.2 W m⁻² to 0.14 W m⁻²



and 0.17 °C to 0.12 °C in equilibrium, respectively. Uncertainty in the climate feedback parameter should also be considered in this estimate. Using a feedback parameter equivalent to that of CO₂, the AR6 likely range for ECS of 2.5-4.0 °C (which may both be oversimplistic assumptions), and 2xCO₂ forcing of 3.9±0.5 W m⁻² (90% range) would produce an equilibrium warming due to a forcing of 0.14 W m⁻² of 0.09-0.14 °C (90% range). Seven years, the timescale used by Yuan et al. (2024) in their calculation, is approximately the time taken for the upper-ocean to reach equilibrium, so, based on Gregory et al. (2024), one would expect to see around two thirds of the equilibrium response (i.e. 0.06-0.10 °C) in that time. With these factors taken into account, the estimate presented by Yuan et al. (2024) would have been consistent with those of Gettelman et al. (2024), and those presented in this work.

ESM estimates of the temperature response to the IMO regulations initially appear to show similar diversity to those based on EBMs. However, this can be seen to largely be due to a difference in the framing of the experiments and reporting of the results, rather than a substantive difference in the main conclusions. Using HadGEM3-GC3.1-LL, Yoshioka et al. (2024) estimated a global mean warming of 0.04 °C (averaged over 2020-2049), which is in agreement with our estimate of 0.03 [-0.09,0.19] °C (averaged over 2020-2040). Their model has a similar ERF of 0.13 Wm⁻², and they use coupled transient simulations with 12 ensemble members per experiment. Their global mean warming estimate is similar to that presented in this study, but the pattern of warming is markedly different, with most of the significant warming over SE Asia and the East Pacific. Conversely, Quaglia & Vioni (2024) estimate a temperature increase of 0.2 °C by 2030 due to the introduction of the IMO regulations. They use the same model that we have used in this study, and a similar experiment design, with transient simulations initialised from the CESM2 Large Ensemble. Although their temperature response is an order of magnitude larger than our stated response, it is not inconsistent with our results. We show in Figure 3a that the global temperature response



280 to the reduction of shipping emissions peaks in 2029 at 0.16 [-0.17, 0.52] °C. Our best estimate of the warming by
281 2030 is 0.07 [-0.14, 0.28] °C, where the range is ± 1 standard deviation and encompasses a warming of 0.2 °C.
282 However, our 18-member ensemble shows that the global ensemble mean warming is not statistically significantly
283 different from zero ($p=0.18$), even in 2030 ($p=0.054$).

284
285 The apparently large discrepancy between our CESM2 numbers and those from Quaglia & Vioni (2024) also
286 demonstrates the importance of framing. We report a 2020-2040 mean value, and they report the value for 2030.
287 Both our Figure 3a and Yoshioka et al. (2024)'s Figure 6 show that the maximum global temperature response to
288 the 2020 emissions change occurs around 2030, and the estimate of the temperature response by 2030 is consistent
289 across all three studies. Yoshioka et al. (2024) also find a long-term mean response of 0.04 °C, averaged over
290 2020-2049, which is more consistent with our estimate of 0.03 °C. However, while we show in Figure 3a that the
291 global warming in response to the IMO regulations is not significant, Yoshioka et al. (2024) present significant
292 decadal mean warming in their Figure 6. However, this is based on ± 1 standard error (SE), while we show ± 1
293 standard deviation. Yoshioka et al. (2024) use 12 members, so their standard deviation of $\sqrt{12} \cdot \text{SE}$ would also
294 indicate that these decadal mean values were always within one standard deviation of 0, consistent with our results.

295
296 Using large ensembles of simulations differing only by the initial conditions is an important technique for
297 distinguishing forced responses from internal variability, particularly when looking for regional responses, or
298 considering small forcings. Here, our large ensemble confirms that the global response to IMO regulations in
299 CESM2 cannot be distinguished from internal variability, at least in terms of global mean surface temperature.
300 Our best estimate is not significantly different from zero, and subsampling our 18-member ensemble to produce
301 estimates of the global temperature response based on different ensemble sizes always returns a mean estimate



302 that is not significantly different from 0 at the 5% level. In fact, given the ensemble variance and the number of
303 simulations available, the minimum detectable effect size over the full 20 years at a significance level of 0.05 is
304 approximately 0.048 °C. The warming due to the ship emissions changes in CESM2 is therefore very likely less
305 than 0.05 °C. A 10-member ensemble, as used by Quaglia & Vioni (2024), can only significantly detect an effect
306 larger than 0.07 °C. To demonstrate this, 10 members sub-sampled from within our 18-member ensemble, can
307 give a global warming estimate of 0.05 °C or a global cooling of 0.05 °C, averaged over 2020-2040.

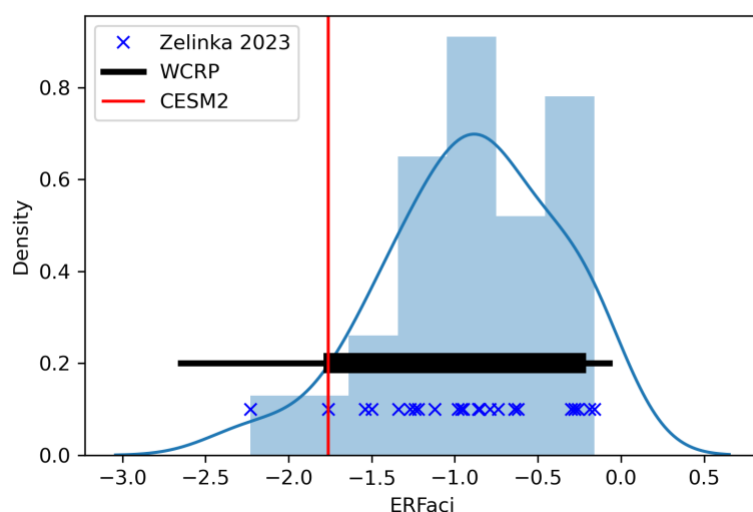
308
309 Large ensembles also make it possible to characterise the spatial pattern of the response, and identify physically
310 robust responses that are consistent across ensemble members. North Atlantic, Greenland Iceland and Norwegian
311 (GIN) seas, South Atlantic, and East Pacific warming are common features of all our subsampled ensembles.
312 However, only the North Atlantic and GIN sea warming are physically robust in addition to being significant at
313 the 5% level. The difference between the pattern of warming shown in this work and by Yoshioka et al. (2024)
314 likely has a large component of internal variability, in addition to the effects of structural differences between the
315 models used.

316
317 Our results highlight the challenge in rapidly attributing observed extreme events to evolving or temporary
318 anthropogenic changes, particularly given the large internal climate variability on annual-to-decadal timescales.
319 By crowd-sourcing computing resources we were able to rapidly generate an ensemble of fully coupled Earth
320 System Model simulations of sufficient size to quantify the forced response and its confidence interval. However,
321 this highlights a deficiency in current medium term climate attribution tasks. As climate change is broadly
322 acknowledged to be increasingly contributing to the extreme events experienced by millions of people around the
323 world, climate scientists are increasingly tasked with understanding and accurately attributing them - but the



resources to conduct this at scale are limited and ad-hoc. An operational climate body that was specifically tasked with running decadal-scale attribution studies (Stevens 2024), or the development of trusted methods for separating forced signals from variability (Samset et al. 2022), would provide a valuable resource as the demand for such information accelerates. The IMO shipping regulations do lead to a relatively small forced global mean surface warming in our results, consistent with its moderate aerosol ERF, and also with a zero response when internal variability is taken into account. However, we note that other, future and ongoing, broader aerosol emission reductions — although uncertain (Persad et al., 2023) — are expected to lead to a much larger aerosol ERF (e.g., Wilcox et al., 2023) and may thus still drive significant global warming and regional climate change impacts (e.g., Allen et al., 2020; Allen et al., 2021).

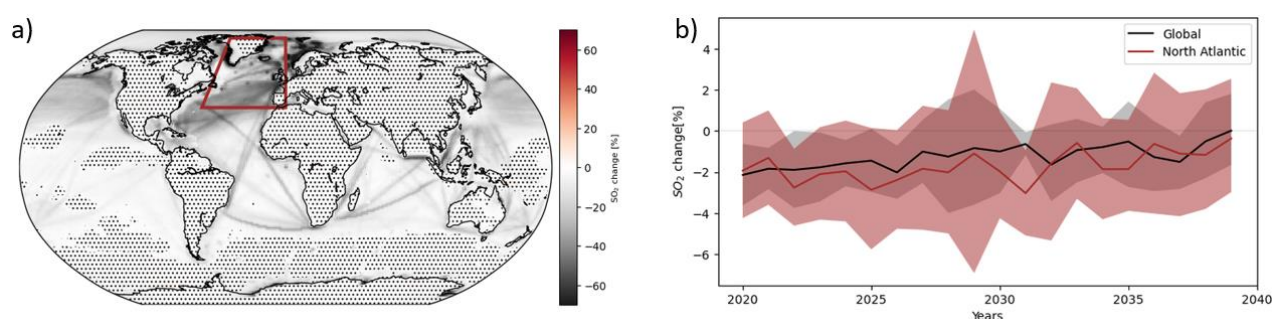
Figures





335 **Figure 1: Distribution of the effective radiative forcing due to aerosol cloud interactions (ERF_{aci}) in CMIP6 models as**
336 **assessed by Zelinka et al. (2023) in blue, and Bellouin et al. 2020 in black, with CESM2 highlighted in red.**

337



338

339 **Figure 2: a) Relative change in SO₂ near the surface due to the shipping emissions perturbation, averaged over the**
340 **whole 2020-2040 period, where stippling represents locations where the null hypothesis of ‘no change’ cannot be**
341 **rejected at $P < 0.05$. b) Annual mean evolution of SO₂, averaged over the entire globe (black line; shading shows +/- one**
342 **standard deviation in ensemble member spread) and over the North Atlantic region (red line) as indicated on the map.**
343 **All changes are relative to the baseline Shared Socioeconomic Pathway 3-7.0 (SSP370).**

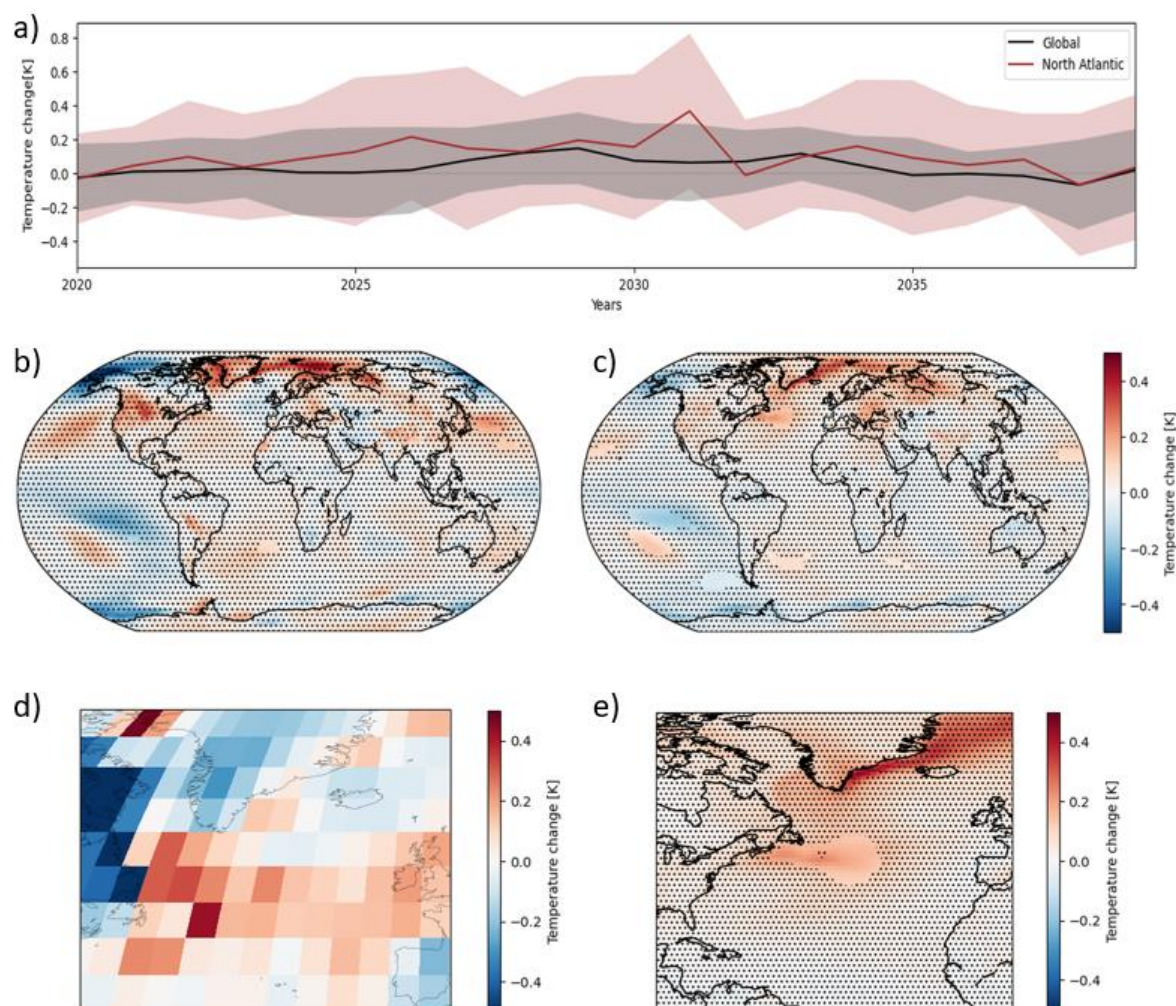
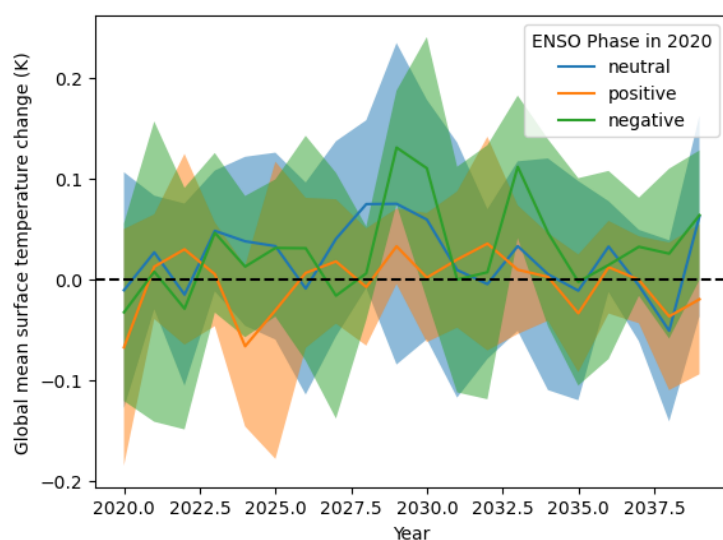


Figure 3: a) Global and North Atlantic annual mean evolution in temperature change (shading shows \pm one standard deviation in ensemble member spread); b) Annual mean temperature change for 2020-2025; c) Annual mean temperature change for 2020-2040; d) Observed anomalous warming in North Atlantic sea-surface temperature in 2023; e) A close-up of (c) showing the corresponding region of the North Atlantic. Stippling in b,c,e represents locations where the null hypothesis of 'no change' cannot be rejected at $P < 0.05$. All changes are relative to the corresponding baseline CESM2 LENS simulations of SSP370.



351



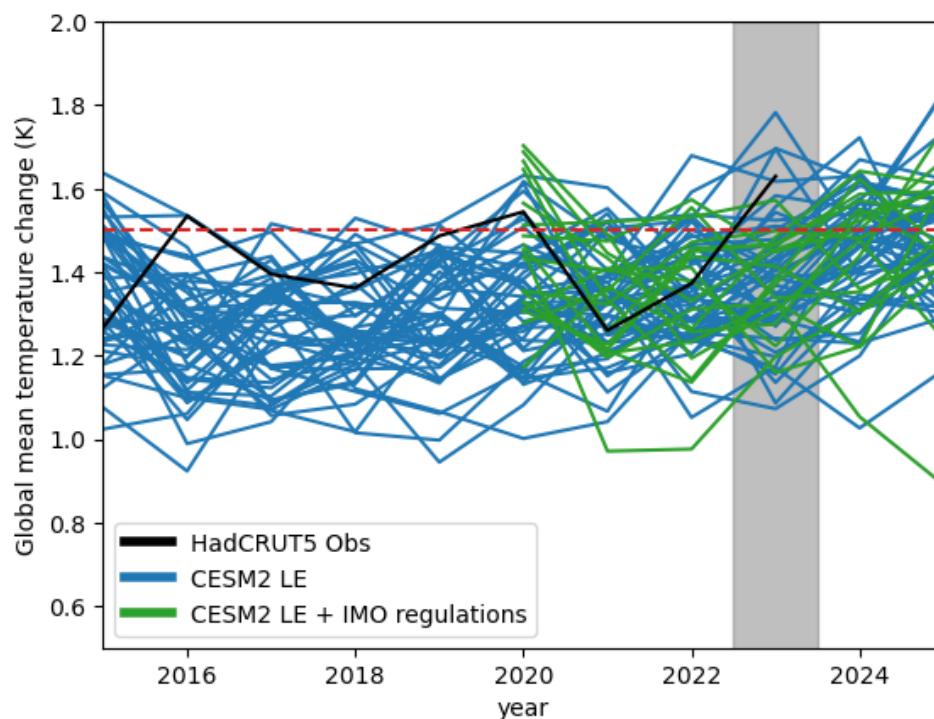
352

353 **Figure 4: Global mean change in surface temperature due to shipping emissions changes with respect to the baseline**

354 **SSP370 simulations, subdivided into three ENSO phases in 2020: neutral (blue; 8 members); positive (orange; 5**

355 **members); negative (green; 5 members). Shading shows the inter-member spread, represented by +/- one standard**

356 **deviation.**



357
358 **Figure 5: Global mean surface temperature change with respect to piControl for the baseline historical + SSP370**
359 **CESM2 LENS ensemble (blue) and the perturbed shipping emissions ensemble performed in this study (green), overlaid**
360 **on the HadCRUT SST observational estimate (with respect to the 1850-1900 average; black). The year 2023 is**
361 **highlighted. The red dashed line represents the 1.5°C Paris agreement warming threshold.**

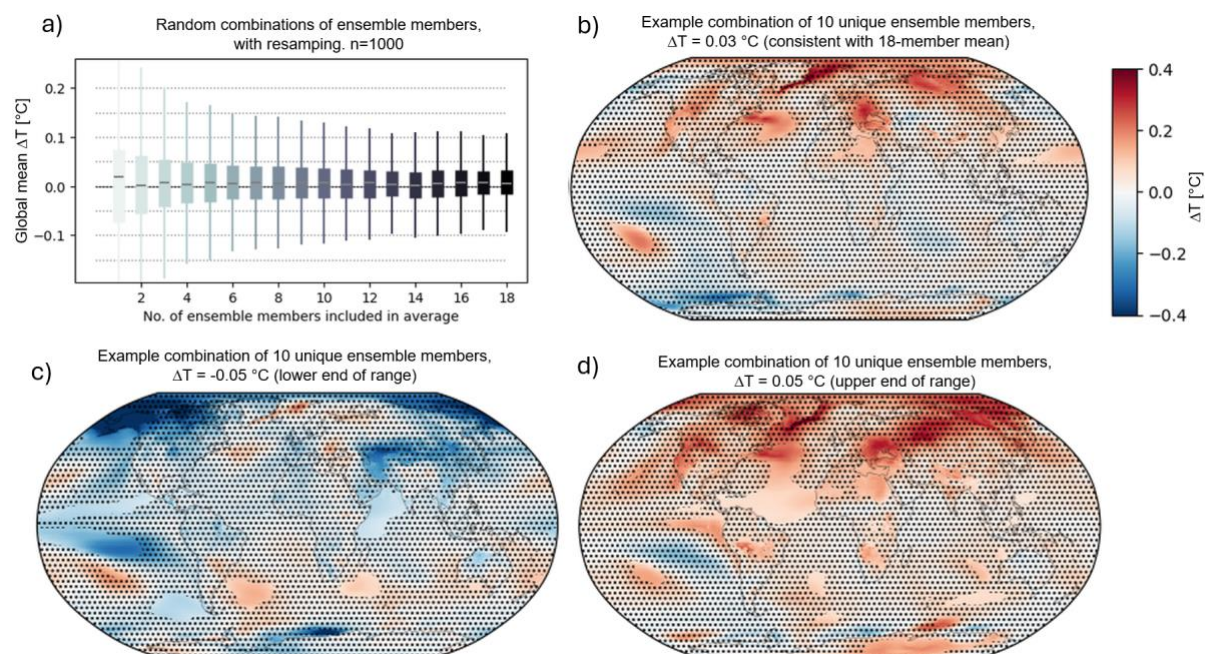


Figure 6: Ensemble size is crucial for quantifying a forced signal for weak perturbations. (a) Spread in 2020-2040 global, annual mean surface temperature change (ΔT) when randomly sampling and averaging N (given on the x-axis) ensemble members out of the total of 18 available members 1000 times, with resampling. Each spread includes 1000 combinations, illustrating an increasing robustness of ΔT as number of ensemble members. Boxes show the median and 5-95% range, whiskers show the maximum and minimum values. (b) Example combination of 10 ensemble members, where the global, annual mean ΔT is consistent with the 18-member mean ($\Delta T = 0.03$ °C). Hatching shows grid points not significant at the 95% confidence level, as for Figure 2. (c) As panel (c), but for an example combination consistent with ΔT at the lower end of the 10-member mean range. ($\Delta T = -0.05$ °C). (d) As panel (c), but for an example combination consistent with ΔT at the upper end of the 10-member mean range. ($\Delta T = 0.05$ °C).



373 **Competing Interests**

374 At least one of the (co-)authors is a member of the editorial board of Atmospheric Chemistry and Physics.
375

376 **Acknowledgements**

377 Part of the simulations were enabled by resources provided by the National Academic Infrastructure for
378 Supercomputing in Sweden (NAISS), partially funded by the Swedish Research Council through grant agreement
379 no. 2022-06725. B.H.S, C.W.S, L.J.W. and M.T.L. acknowledge funding by the Research Council of Norway
380 through projects CATHY (324182), and support by the Center for Advanced Study in Oslo, Norway that funded
381 and hosted the HETCLIF centre during the academic year of 2023/24. C.W.S. is also supported by the Research
382 Council of Norway through the ACCEPT project (315195). G.P acknowledges support from the U.S. National
383 Science Foundation under AGS-CLD Award #2235177. A.M.L.E acknowledges support from the European
384 Union's Horizon 2020 research and innovation programme (FORCeS, grant no. 821205). R.J.A. is supported by
385 NSF grant AGS-2153486. We would like to acknowledge high-performance computing support from Cheyenne
386 (doi:10.5065/D6RX99HX) provided by the NCAR-Wyoming Supercomputing Center, sponsored by the National
387 Science Foundation and the State of Wyoming and supported by NCAR's Computational and Information Systems
388 Laboratory using allocation WYOM0182. The authors are grateful to Jonathan Gregory for discussions that
389 strengthened this manuscript.

390

391

392

393



References

- Albrecht, B. A. (1989). Aerosols, Cloud Microphysics, and Fractional Cloudiness. *Science*, 245(4923), 1227–1230. <https://doi.org/10.1126/science.245.4923.1227>
- Bellouin, N., Quaas, J., Gryspeerdt, E., Kinne, S., Stier, P., Watson-Parris, D., Boucher, O., Carslaw, K. S., Christensen, M., Daniau, A.-L., Dufresne, J.-L., Feingold, G., Fiedler, S., Forster, P., Gettelman, A., Haywood, J. M., Lohmann, U., Malavelle, F., Mauritsen, T., ... Stevens, B. (2020). Bounding Global Aerosol Radiative Forcing of Climate Change. *Reviews of Geophysics*, 58(1), e2019RG000660. <https://doi.org/10.1029/2019RG000660>
- Bogenschütz, P. A., Gettelman, A., Hannay, C., Larson, V. E., Neale, R. B., Craig, C., & Chen, C.-C. (2018). The path to CAM6: coupled simulations with CAM5.4 and CAM5.5. *Geoscientific Model Development*, 11(1), 235–255. <https://doi.org/10.5194/gmd-11-235-2018>
- Burney, J., Persad, G., Proctor, J., Bendavid, E., Burke, M., & Heft-Neal, S. (2022). Geographically resolved social cost of anthropogenic emissions accounting for both direct and climate-mediated effects. *Science Advances*, 8(38), eabn7307. <https://doi.org/10.1126/sciadv.abn7307>
- Christensen, M. W., Gettelman, A., Cermak, J., Dagan, G., Diamond, M., Douglas, A., Feingold, G., Glassmeier, F., Goren, T., Grosvenor, D. P., Gryspeerdt, E., Kahn, R., Li, Z., Ma, P. L., Malavelle, F., McCoy, I. L.,



- 416 McCoy, D. T., McFarquhar, G., Mülmenstädt, J., ... Yuan, T. (2022). Opportunistic experiments to constrain
417 aerosol effective radiative forcing. *Atmospheric Chemistry and Physics*, 22(1), 641–674.
418 <https://doi.org/10.5194/acp-22-641-2022>
- 419 Danabasoglu, G., Bates, S. C., Briegleb, B. P., Jayne, S. R., Jochum, M., Large, W. G., Peacock, S., & Yeager, S.
420 G. (2012). The CCSM4 Ocean Component. *Journal of Climate*, 25(5), 1361–1389.
421 <https://doi.org/10.1175/JCLI-D-11-00091.1>
- 422 Danabasoglu, G., Lamarque, J.-F., Bacmeister, J., Bailey, D. A., DuVivier, A. K., Edwards, J., Emmons, L. K.,
423 Fasullo, J., Garcia, R., Gettelman, A., Hannay, C., Holland, M. M., Large, W. G., Lauritzen, P. H., Lawrence,
424 D. M., Lenaerts, J. T. M., Lindsay, K., Lipscomb, W. H., Mills, M. J., ... Strand, W. G. (2020). The
425 Community Earth System Model Version 2 (CESM2). *Journal of Advances in Modeling Earth Systems*,
426 12(2), e2019MS001916. <https://doi.org/10.1029/2019MS001916>
- 427 Deser, C., Knutti, R., Solomon, S., & Phillips, A. S. (2012). Communication of the role of natural variability in
428 future North American climate. *Nature Climate Change*, 2(11), 775–779.
429 <https://doi.org/10.1038/nclimate1562>
- 430 Deser, C., Lehner, F., Rodgers, K. B., Ault, T., Delworth, T. L., DiNezio, P. N., Fiore, A., Frankignoul, C., Fyfe,
431 J. C., Horton, D. E., Kay, J. E., Knutti, R., Lovenduski, N. S., Marotzke, J., McKinnon, K. A., Minobe, S.,
432 Randerson, J., Screen, J. A., Simpson, I. R., & Ting, M. (2020). Insights from Earth system model initial-
433 condition large ensembles and future prospects. *Nature Climate Change*, 10(4), 277–286.
434 <https://doi.org/10.1038/s41558-020-0731-2>
- 435 Diamond, M. S. (2023). Detection of large-scale cloud microphysical changes within a major shipping corridor
436 after implementation of the International Maritime Organization 2020 fuel sulfur regulations. *Atmospheric
437 Chemistry and Physics*, 23(14), 8259–8269. <https://doi.org/10.5194/acp-23-8259-2023>



- 438 Emmons, L. K., Schwantes, R. H., Orlando, J. J., Tyndall, G., Kinnison, D., Lamarque, J.-F., Marsh, D., Mills, M.
439 J., Tilmes, S., Bardeen, C., Buchholz, R. R., Conley, A., Gettelman, A., Garcia, R., Simpson, I., Blake, D.
440 R., Meinardi, S., & Pétron, G. (2020). The Chemistry Mechanism in the Community Earth System Model
441 Version 2 (CESM2). *Journal of Advances in Modeling Earth Systems*, 12(4), e2019MS001882.
442 <https://doi.org/10.1029/2019MS001882>
- 443 Fasullo, J. T., Lamarque, J.-F., Hannay, C., Rosenbloom, N., Tilmes, S., DeRepentigny, P., Jahn, A., & Deser, C.
444 (2022). Spurious Late Historical-Era Warming in CESM2 Driven by Prescribed Biomass Burning
445 Emissions. *Geophysical Research Letters*, 49(2), e2021GL097420. <https://doi.org/10.1029/2021GL097420>
- 446 Fasullo, J. T., Rosenbloom, N., & Buchholz, R. (2023). A multiyear tropical Pacific cooling response to recent
447 Australian wildfires in CESM2. *Science Advances*, 9(19), eadg1213. <https://doi.org/10.1126/sciadv.adg1213>
- 448 Forster, P., Storelvmo, T., Armour, K., Collins, W., Dufresne, J.-L., Frame, D., Lunt, D., Mauritsen, T., Palmer,
449 M., & Watanabe, M. (2021). The Earth's energy budget, climate feedbacks, and climate sensitivity. *Climate*
450 *Change 2021: The Physical Science Basis. Contribution of Working Group I to the Sixth Assessment Report*
451 *of the Intergovernmental Panel on Climate Change*, 923–1054. <https://doi.org/10.1017/9781009157896.009>
- 452 Gettelman, A., & Morrison, H. (2015). Advanced Two-Moment Bulk Microphysics for Global Models. Part I:
453 Off-Line Tests and Comparison with Other Schemes. *Journal of Climate*, 28(3), 1268–1287.
454 <https://doi.org/10.1175/JCLI-D-14-00102.1>
- 455 Gettelman, A., Christensen, M. W., Diamond, M. S., Gryspeerdt, E., Manshausen, P., Stier, P., Watson-Parris,
456 D., Yang, M., Yoshioka, M., Yuan, T.: Has Reducing Ship Emissions Brought Forward Global Warming?
457 *Geophysical Review Letters* (under review)



- 458 Glassmeier, F., Hoffmann, F., Johnson, J. S., Yamaguchi, T., Carslaw, K. S., & Feingold, G. (2021). Aerosol-
459 cloud-climate cooling overestimated by ship-track data. *Science*, 371(6528), 485–489.
460 <https://doi.org/doi:10.1126/science.abd3980>
- 461 Hassan, T., Allen, R. J., Liu, W., & Randles, C. A. (2021). Anthropogenic aerosol forcing of the Atlantic
462 meridional overturning circulation and the associated mechanisms in CMIP6 models. *Atmospheric*
463 *Chemistry and Physics*, 21(8), 5821–5846. <https://doi.org/10.5194/acp-21-5821-2021>
- 464 Hunke, E. C., Lipscomb, W. H., Turner, A. K., Jeffery, N., & Elliott, S. (2015). CICE: the Los Alamos Sea Ice
465 Model Documentation and Software User’s Manual Version 5. *Los Alamos National Laboratory Technical*
466 *Report, LA-CC-06-012*.
- 467 IMO: IMO 2020: Consistent Implementation of MARPOL Annex VI. International Maritime Organization, 2019
- 468 Kay, J. E., Deser, C., Phillips, A., Mai, A., Hannay, C., Strand, G., Arblaster, J. M., Bates, S. C., Danabasoglu, G.,
469 Edwards, J., Holland, M., Kushner, P., Lamarque, J.-F., Lawrence, D., Lindsay, K., Middleton, A., Munoz,
470 E., Neale, R., Oleson, K., ... Vertenstein, M. (2015). The Community Earth System Model (CESM) Large
471 Ensemble Project: A Community Resource for Studying Climate Change in the Presence of Internal Climate
472 Variability. *Bulletin of the American Meteorological Society*, 96(8), 1333–1349.
473 <https://doi.org/10.1175/BAMS-D-13-00255.1>
- 474 Kirchmeier-Young, M. C., Zwiers, F. W., & Gillett, N. P. (2017). Attribution of Extreme Events in Arctic Sea Ice
475 Extent. *Journal of Climate*, 30(2), 553–571. <https://doi.org/10.1175/JCLI-D-16-0412.1>
- 476 Lawrence, D. M., Fisher, R. A., Koven, C. D., Oleson, K. W., Swenson, S. C., Bonan, G., Collier, N., Ghimire,
477 B., van Kampenhout, L., Kennedy, D., Kluzek, E., Lawrence, P. J., Li, F., Li, H., Lombardozzi, D., Riley,
478 W. J., Sacks, W. J., Shi, M., Vertenstein, M., ... Zeng, X. (2019). The Community Land Model Version 5:



- 479 Description of New Features, Benchmarking, and Impact of Forcing Uncertainty. *Journal of Advances in*
480 *Modeling Earth Systems*, 11(12), 4245–4287. <https://doi.org/10.1029/2018MS001583>
- 481 Li, C., McLinden, C., Fioletov, V., Krotkov, N., Carn, S., Joiner, J., Streets, D., He, H., Ren, X., Li, Z., &
482 Dickerson, R. R. (2017). India Is Overtaking China as the World’s Largest Emitter of Anthropogenic Sulfur
483 Dioxide. *Scientific Reports*, 7(1), 14304. <https://doi.org/10.1038/s41598-017-14639-8>
- 484 Liu, X., Ma, P. L., Wang, H., Tilmes, S., Singh, B., Easter, R. C., Ghan, S. J., & Rasch, P. J. (2016). Description
485 and evaluation of a new four-mode version of the Modal Aerosol Module (MAM4) within version 5.3 of the
486 Community Atmosphere Model. *Geoscientific Model Development*, 9(2), 505–522.
487 <https://doi.org/10.5194/gmd-9-505-2016>
- 488 Ma, X., Liu, W., Allen, R. J., Huang, G., & Li, X. (2020). Dependence of regional ocean heat uptake on
489 anthropogenic warming scenarios. *Science Advances*, 6(45). <https://doi.org/10.1126/sciadv.abc0303>
- 490 Maher, N., Milinski, S., Suarez-Gutierrez, L., Botzet, M., Dobrynin, M., Kornblueh, L., Kröger, J., Takano, Y.,
491 Ghosh, R., Hedemann, C., Li, C., Li, H., Manzini, E., Notz, D., Putrasahan, D., Boysen, L., Claussen, M.,
492 Ilyina, T., Olonscheck, D., ... Marotzke, J. (2019). The Max Planck Institute Grand Ensemble: Enabling the
493 Exploration of Climate System Variability. *Journal of Advances in Modeling Earth Systems*, 11(7), 2050–
494 2069. <https://doi.org/10.1029/2019MS001639>
- 495 Monerie, P.-A., Wilcox, L. J., & Turner, A. G. (2022). Effects of Anthropogenic Aerosol and Greenhouse Gas
496 Emissions on Northern Hemisphere Monsoon Precipitation: Mechanisms and Uncertainty. *Journal of*
497 *Climate*, 35(8), 2305–2326. <https://doi.org/10.1175/JCLI-D-21-0412.1>
- 498 Morice, C. P., Kennedy, J. J., Rayner, N. A., Winn, J. P., Hogan, E., Killick, R. E., Dunn, R. J. H., Osborn, T. J.,
499 Jones, P. D., & Simpson, I. R. (2021). An Updated Assessment of Near-Surface Temperature Change From



- 500 1850: The HadCRUT5 Data Set. *Journal of Geophysical Research: Atmospheres*, 126(3).
501 <https://doi.org/10.1029/2019JD032361>
- 502 O'Neill, B. C., Tebaldi, C., Vuuren, D. P. van, Eyring, V., Friedlingstein, P., Hurtt, G., Knutti, R., Kriegler, E.,
503 Lamarque, J.-F., Lowe, J., Meehl, G. A., Moss, R., Riahi, K., & Sanderson, B. M. (2016). The Scenario
504 Model Intercomparison Project (ScenarioMIP) for CMIP6. *Geoscientific Model Development*, 9(9), 3461–
505 3482. <https://doi.org/10.5194/gmd-9-3461-2016>
- 506 Persad, G. G., & Caldeira, K. (2018). Divergent global-scale temperature effects from identical aerosols emitted
507 in different regions. *Nat Commun*, 9(1), 3289. <https://doi.org/10.1038/s41467-018-05838-6>
- 508 Quaglia, I., & Vioni, D. (2024). Modeling 2020 regulatory changes in international shipping emissions helps
509 explain 2023 anomalous warming. *EGUsphere*, 1–19. <https://doi.org/10.5194/egusphere-2024-1417>
- 510 Rodgers, K. B., Lee, S.-S., Rosenbloom, N., Timmermann, A., Danabasoglu, G., Deser, C., Edwards, J., Kim, J.-
511 E., Simpson, I. R., Stein, K., Stuecker, M. F., Yamaguchi, R., Bódai, T., Chung, E.-S., Huang, L., Kim, W.
512 M., Lamarque, J.-F., Lombardozzi, D. L., Wieder, W. R., & Yeager, S. G. (2021). Ubiquity of human-
513 induced changes in climate variability. *Earth System Dynamics*, 12(4), 1393–1411.
514 <https://doi.org/10.5194/esd-12-1393-2021>
- 515 Samset, B. H., Lund, M. T., Bollasina, M., Myhre, G., & Wilcox, L. (2019). Emerging Asian aerosol patterns.
516 *Nature Geoscience*, 12(8), 582–584. <https://doi.org/10.1038/s41561-019-0424-5>
- 517 Schlund, M., Lauer, A., Gentine, P., Sherwood, S. C., & Eyring, V. (2020). Emergent constraints on equilibrium
518 climate sensitivity in CMIP5: do they hold for CMIP6? *Earth System Dynamics*, 11(4), 1233–1258.
519 <https://doi.org/10.5194/esd-11-1233-2020>
- 520 Schmidt, G. (2024). Climate models can't explain 2023's huge heat anomaly — we could be in uncharted territory.
521 *Nature*, 627(8004), 467. <https://doi.org/10.1038/d41586-024-00816-z>



- 522 Shindell, D., & Faluvegi, G. (2009). Climate response to regional radiative forcing during the twentieth century.
523 *Nature Geoscience*, 2(4), 294–300. <https://doi.org/10.1038/ngeo473>
- 524 Simpson, I. R., Rosenbloom, N., Danabasoglu, G., Deser, C., Yeager, S. G., McCluskey, C. S., Yamaguchi, R.,
525 Lamarque, J.-F., Tilmes, S., Mills, M. J., & Rodgers, K. B. (2023). The CESM2 Single-Forcing Large
526 Ensemble and Comparison to CESM1: Implications for Experimental Design. *Journal of Climate*, 36(17),
527 5687–5711. <https://doi.org/10.1175/JCLI-D-22-0666.1>
- 528 Skeie, R. B., Byrom, R., Hodnebrog, Ø., Jouan, C., & Myhre, G. (2024). Multi-model effective radiative forcing
529 of the 2020 sulphur cap for shipping. *EGUsphere*, 1–14. <https://doi.org/10.5194/egusphere-2024-1394>
- 530 Stevens, B., & Feingold, G. (2009). Untangling aerosol effects on clouds and precipitation in a buffered system.
531 *Nature*, 461(7264), 607–613. <https://doi.org/10.1038/nature08281>
- 532 Twomey, S. (1974). Pollution and the planetary albedo. *Atmospheric Environment* (1967), 8(12), 1251–1256.
533 <http://www.sciencedirect.com/science/article/pii/0004698174900043>
- 534 van der A, R. J., Mijling, B., Ding, J., Koukouli, M. E., Liu, F., Li, Q., Mao, H., & Theys, N. (2017). Cleaning up
535 the air: effectiveness of air quality policy for SO₂ and NO_x emissions in China. *Atmospheric Chemistry and*
536 *Physics*, 17(3), 1775–1789. <https://doi.org/10.5194/acp-17-1775-2017>
- 537 Wall, C. J., Norris, J. R., Possner, A., McCoy, D. T., McCoy, I. L., & Lutsko, N. J. (2022). Assessing effective
538 radiative forcing from aerosol–cloud interactions over the global ocean. *Proceedings of the National*
539 *Academy of Sciences*, 119(46), e2210481119. <https://doi.org/10.1073/pnas.2210481119>
- 540 Wang, G., Cai, W., Santoso, A., Wu, L., Fyfe, J. C., Yeh, S.-W., Ng, B., Yang, K., & McPhaden, M. J. (2022).
541 Future Southern Ocean warming linked to projected ENSO variability. *Nature Climate Change*, 12(7), 649–
542 654. <https://doi.org/10.1038/s41558-022-01398-2>



- 543 Watson-Parris, D., Christensen, M. W., Laurenson, A., Clewley, D., Gryspeerdt, E., & Stier, P. (2022). Shipping
544 regulations lead to large reduction in cloud perturbations. *Proceedings of the National Academy of Sciences*,
545 119(41), e2206885119. <https://doi.org/10.1073/pnas.2206885119>
- 546 Watson-Parris, D., & Smith, C. J. (2022). Large uncertainty in future warming due to aerosol forcing. *Nature*
547 *Climate Change*, 12(12), 1111–1113. <https://doi.org/10.1038/s41558-022-01516-0>
- 548 Westervelt, D. M., Mascioli, N. R., Fiore, A. M., Conley, A. J., Lamarque, J.-F., Shindell, D. T., Faluvegi, G.,
549 Previdi, M., Correa, G., & Horowitz, L. W. (2020). Local and remote mean and extreme temperature
550 response to regional aerosol emissions reductions. *Atmospheric Chemistry and Physics*, 20(5), 3009–3027.
551 <https://doi.org/https://doi.org/10.5194/acp-20-3009-2020>
- 552 Yoshioka, M., Grosvenor, D. P., Booth, B. B. B., Morice, C. P., & Carslaw, K. S. (2024). Warming effects of
553 reduced sulfur emissions from shipping. *EGUsphere*, 1–19. <https://doi.org/10.5194/egusphere-2024-1428>
- 554 Yuan, T., Song, H., Oreopoulos, L., Wood, R., Bian, H., Breen, K., Chin, M., Yu, H., Barahona, D., Meyer, K., &
555 Platnick, S. (2024). Abrupt reduction in shipping emission as an inadvertent geoengineering termination
556 shock produces substantial radiative warming. *Communications Earth & Environment*, 5(1), 1–8.
557 <https://doi.org/10.1038/s43247-024-01442-3>
- 558 Zelinka, M. D., Smith, C. J., Qin, Y., & Taylor, K. E. (2023). Comparison of methods to estimate aerosol effective
559 radiative forcings in climate models. *Atmospheric Chemistry and Physics*, 23(15), 8879–8898.
560 <https://doi.org/10.5194/acp-23-8879-2023>
- 561
- 562
- 563